

Supplemental information

Methods

Cell culture, flow cytometry, venetoclax sensitivity assay and synergy experiment

Peripheral blood mononuclear cells (PBMCs) of CLL patients were submitted to CD40 activation by being co-cultured with NIH3T3 fibroblasts stably transfected with human CD40L or negative control in presence or not of the following inhibitors: 4 μ M 2DG, 5nM/10nM Oligomycin, 20 μ M DON, 2 μ M UK5099, 4 μ M etomoxir, 100nM Rotenone, 10mM DMM, 1 μ M Antimycin A, 500nM/250nM AZD8055, 1 μ M/500nM Rapamycin, 10 μ M/50 μ M MYLS22, 100nM Idelalisib, 2,5 μ M MK2206 or 100nM Ibrutinib. Drugs concentration have been determined by titration or following concentration used in the Seahorse set up avoiding decreased basal viability of CLL cells. Moreover, CD40L expression on NIH3T3 fibroblasts is not altered in presence of these drugs concentration. After 24 hours, CLL cells were gently detached from fibroblasts and stained with a viability dye and for CD95 and CD40L surface expression. Cells were subsequently permeabilized and stained with anti MCL1, BCL-XL and BCL2 proteins. For metabolic determinations by flow cytometry, cells were stained with 2-(N-(7-Nitrobenz-2-oxa-1, 3-diazol-4-yl) Amino)-2-Deoxyglucose (2-NBDG) and Mito Tracker green FM to assess glucose uptake and mitochondrial mass, respectively. For venetoclax sensitivity assays, cells were harvested from fibroblasts co-cultures and incubated with increasing concentrations of venetoclax for an additional 24 hours. CLL cell viability was measured by flow cytometry using MitoTracker Orange or DioC6 and TO-PRO-3. Stained cells were analyzed on a FACS Canto II cytometer (BD Biosciences, San Jose, CA, USA). Data analysis was performed using FlowJo v9.7.6 (FlowJo, Ashland, OR, USA). Specific apoptosis is defined as [% cell death in treated cells] – [% cell death in medium control] / [% viable cells medium control] x 100^{1,2}.

Combination index was calculated as followed, IC50 values calculated using a nonlinear regression model^{1,3}: Calculations were done for 3T40-activated CLL cells. IC50 values for single treatments were not achieved (NA), IC50 values for dual treatments were calculated from Figure 5A and triple treatment in 3T40L CLL cells were calculated from Supplemental Figure S6A.

Microarrays

As described before, this dataset has been already published⁴. Samples from 3 CLL patients were stimulated for 16h with either NIH3T3 fibroblasts stably transfected with human CD40L or negative control, CLL cells were sorted to >99% purity using CD5/CD19 staining (FACS ARIA, BD Biosciences, San Jose, CA, USA) and analyzed on a FACS Canto II cytometer (BD Biosciences, San Jose, CA, USA). Total RNA from these samples was isolated by using TriReagent according to manufacturer's instructions and RNA was further purified using the RNeasy micro kit according to manufacturer's instructions including DNase treatment. RNA was then hybridized on a U133plus2 microarray chip (Affymetrix, Santa Clara, CA, USA). The experiments were analyzed using Bioconductor packages in the statistical software package R (version 3.1.2). Raw data were extracted from the CEL files using the package affy. Lists of genes involving OXPHOS or glycolysis were selected from KEGG database, then the expression of these genes was visualized by heat maps with Z-score on Tercen (www.tercen.com).

Metabolic assays

Oxygen consumption rate (OCR) and extracellular acidification rate (ECAR) were measured by Mito Stress tests in a XF96 Extracellular Flux Analyzer (Agilent, Santa Clara, CA, USA),

according to manufacturer's instructions. After CD40 stimulation with or without inhibitors, lymphocytes of CLL patients were resuspended in RPMI assay medium supplemented with 10 mM glucose, 1 mM pyruvate and 2 mM glutamine. 200,000 cells/well were plated in XF96 plates pre-coated with Poly-D-Lysine at 50µg/mL and centrifuged to immobilize cells at the bottom of the wells. XF plates were incubated in a non-CO₂ incubator at 37 °C for 2hr to equilibrate the temperature. Oxygen consumption was monitored under basal conditions and in response to 1µM oligomycin (final concentration), 0,5µM carbonyl cyanide p-trifluoromethoxyphenylhydrazone (FCCP), 0,75µM rotenone, and 1,5µM antimycin A. The basal respiration rate was calculated as the difference between basal OCR and the OCR after inhibition of mitochondrial complexes I and III with rotenone and antimycin A, respectively. Spare respiratory capacity was measured by the difference between the maximal OCR and basal OCR. ATP and NAD⁺/NADH levels were measured according to the standard procedures of the ATPlite kit and NAD⁺/NADH kit, respectively.

Western blot analysis

Western blot analysis was performed using standard techniques. Cells were lysed in RIPA buffer containing 50 mM TrisHCl pH7.4, 150 mM NaCl, 1 mM EDTA pH 8, 0.1% SDS, 1% NP-40, plus a protease and a phosphatase inhibitor cocktail. After a 30-min incubation on ice, extracts were centrifuged, and supernatants were harvested. Protein lysates (30µg) were resolved on SDS–polyacrylamide gels (13%) and transferred electrophoretically onto polyvinylidene difluoride (PVDF) membranes. PVDF membranes were incubated with the following antibodies: CD40, actin, P-AKT^{S473}, P-AKT^{T450}, P-GSK-3B^{S9}, P-eIF2a^{S51}. Odyssey Imager (Li-Cor Biosciences, Lincoln, NE, USA) was used as a detection method according to

the manufacturer's protocol. Quantification of western blot bands was performed on Image J (NIH, Bethesda, MD, USA), the average intensities of the bands were calculated.

Real-time polymerase chain reaction

Total RNA was isolated using the RNeasy kit according to the manufacturer's instructions and converted to cDNA using oligo(dT) primers and RevertAid H Minus M-MuLV Reverse Transcriptase. mRNA expression was quantified by quantitative PCR (Q-PCR) using a QuantStudio 3 Real-Time PCR System (Thermo Fisher Scientific, Waltham, MA, USA) and a Fast SYBR green reaction Mix and the probes for CD40, alternative spliced CD40 and CELF1 (Table S3). Relative RNA quantities were calculated with the equation $RQ=2^{-(\Delta\Delta CT)}$ using TBP expression as an internal control (housekeeping gene).

Protein translation assay

Click-iT assays were performed using $0,5 \cdot 10^6$ cells per assay. O-propargyl l-puromycin (OPP; 20 μ M final concentration) (Life Technologies) was added to the cells and incubated for 30 minutes at 37C. Cells were washed in ice-cold PBS and then fixed and permeabilized using the Cytofix/Cytoperm Fixation Permeabilization Kit. Alexa-Fluor-488 was conjugated to OPP as described in the manufacturer's instructions and cells were stained with anti-CD5 and anti-CD19 antibodies for 20 minutes at 4C. Cells were washed in Cytoperm buffer and resuspended in PBS 0,5% BSA before data acquisition using a FACS Canto II cytometer (BD Biosciences, San Jose, CA, USA). Data analysis was performed using FlowJo v9.7.6 (FlowJo, Ashland, OR, USA). As a control, a proportion of cells were treated with cycloheximide for 5 minutes before OPP addition and fluorescence of cycloheximide-treated cells was subtracted from all experimental values.

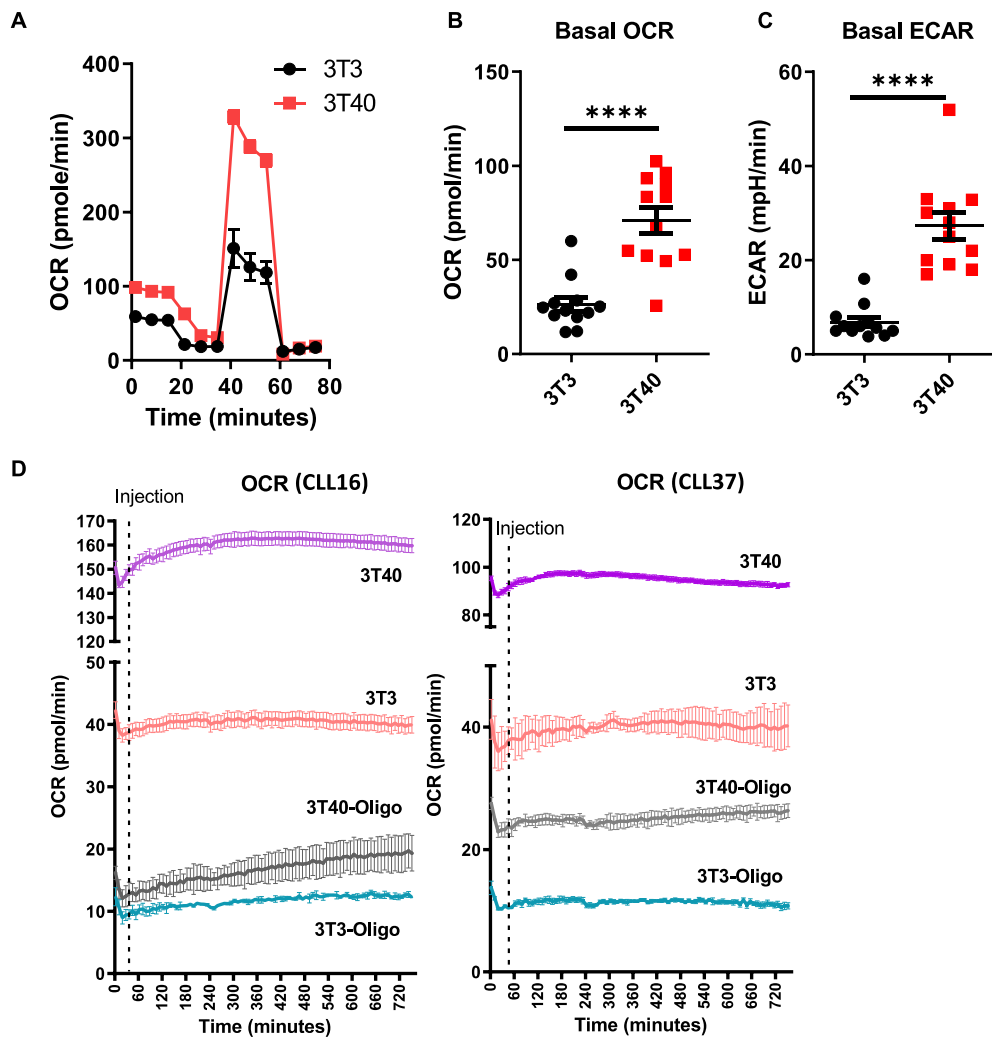


Figure S1. CD40 stimulation enhances metabolic activity of CLL cells (A) A representative Seahorse MitoStress test after CLL cells were cultured on 3T3 or 3T40 fibroblasts for 48 hours. (B) Basal OCR and (C) Basal ECAR were measured (n=12). Data are shown as mean \pm SEM. Paired T-test was performed to compare 3T3 and 3T40 condition. (D) CLL cells were cultured on 3T3 or 3T40 and simultaneously treated with/without oligomycin for 24 hours. After resuspension, CLL cells were seeded on Seahorse plate, OCR was measured every 8 minutes. After 4 measurements, 10 nM Venetoclax were injected into the cells, then OCR was measured every 8 minutes for 750 minutes.

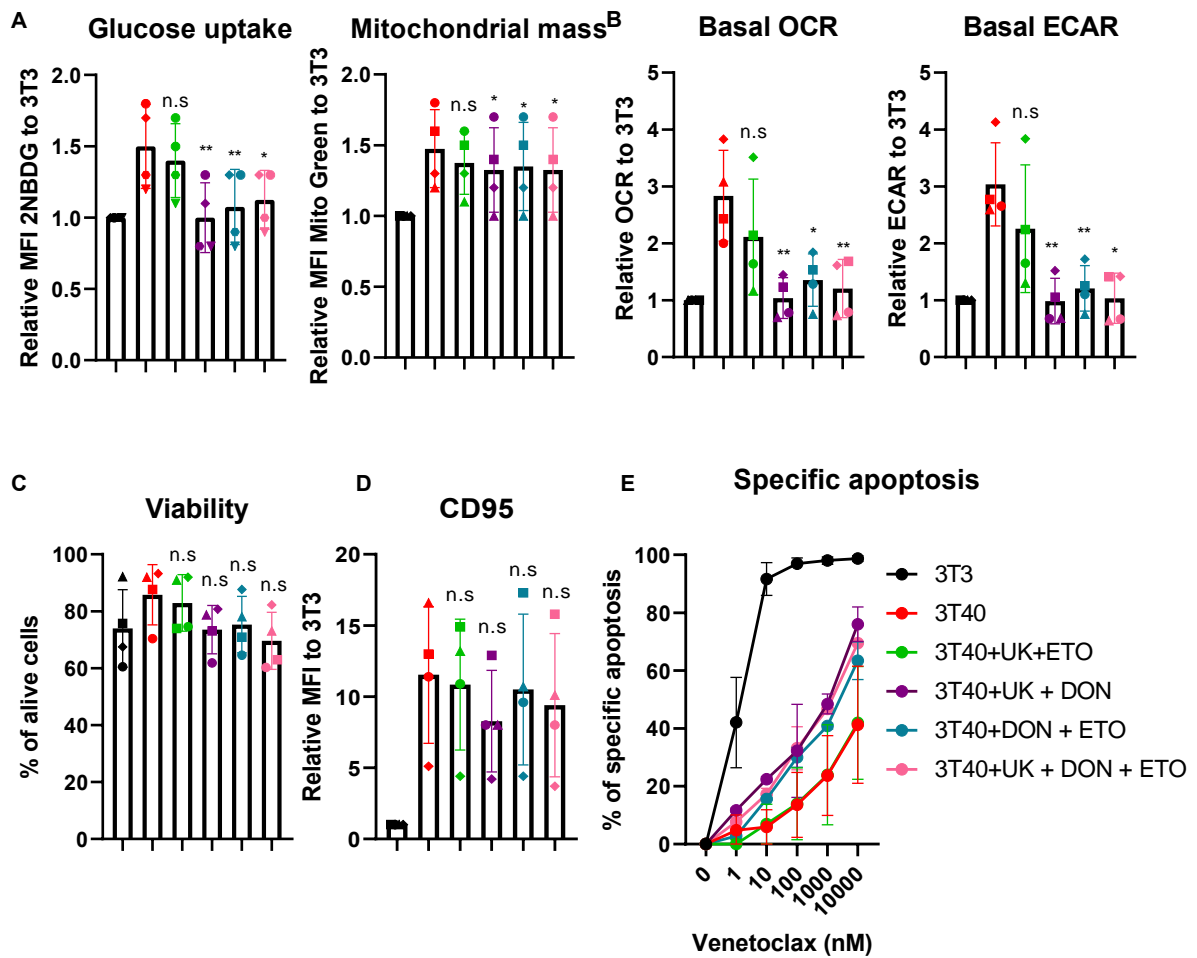


Figure S2. Inhibition of 3 main fuels of TCA cycle impairs CLL metabolism but not the sensitivity to venetoclax. CLL cells (n=4) were cultured on 3T3 or 3T40 fibroblasts and simultaneously treated with 2 μ M UK5099+4 μ M etomoxir, 2 μ M UK5099+20 μ M DON, 20 μ M DON + 4 μ M etomoxir or 2 μ M UK5099+ 20 μ M DON+4 μ M etomoxir for 24 hours. After resuspension, (A) glucose uptake and mitochondrial mass were measured by flow cytometry. A Seahorse MitoStress test was performed, (B) basal OCR and basal ECAR were measured and calculated on Seahorse XF96 analyser. (C) Viability and (D) CD95 expression was measured by flow cytometry. (E) After resuspension, CLL cells were also incubated with a titration of 1-10000 nM venetoclax for 24 hours after which viability was measured using DiOC6 and TO-PRO-3. Then specific apoptosis was calculated (n=4). Data are shown as mean \pm SEM. One-Way ANOVA was performed to compare 3T40 to the other conditions. Each patient is labelled with a distinct symbol across all the conditions.

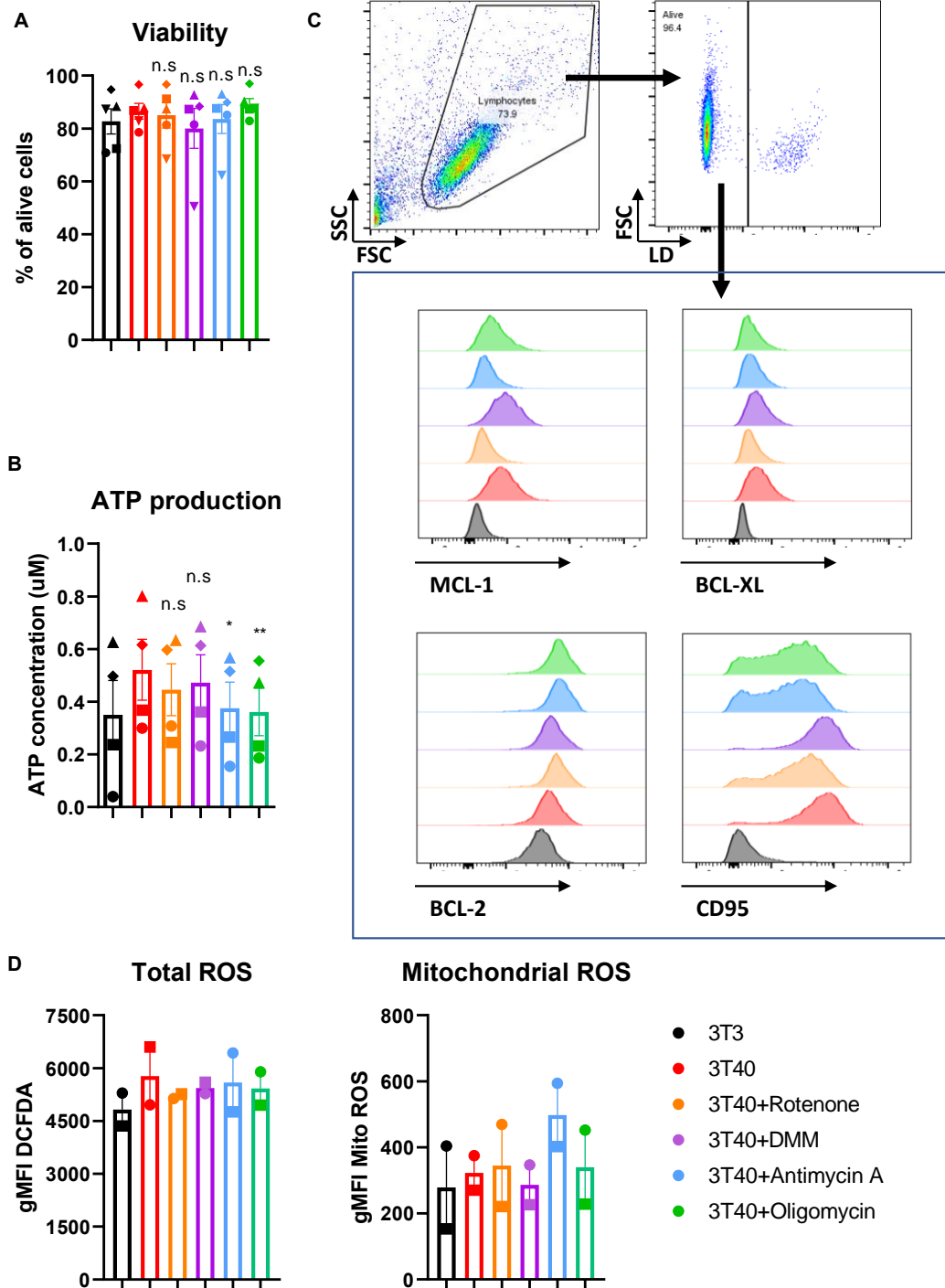


Figure S3. Effects of ETC inhibition on ROS, ATP and NAD production. CLL cells were cultured on 3T3 or 3T40 fibroblasts and simultaneously treated with ETC inhibitors for 24 hours. After resuspension, (A) Viability of the cells were measured by flow cytometer with Dio6/ToPro3 staining (n=5). (B) ATP production was measured by a commercial kit (n=4). (C) Details of measurement of BCL-2 family members and CD95 by flow cytometer. CLL cells were gated by forward scatter and sideward scatter, after define the viable cells by V780 staining, expression of BCL-2 family members and CD95 were evaluated in viable cells. The histograms show the expression of each protein in various conditions. (D) Total ROS and mitochondrial ROS were measured by flow cytometry (n=2). Data are shown as mean +/- SEM. One-Way ANOVA was performed to compare 3T40 to the other conditions. Each patient is labelled with a distinct symbol across all the conditions.

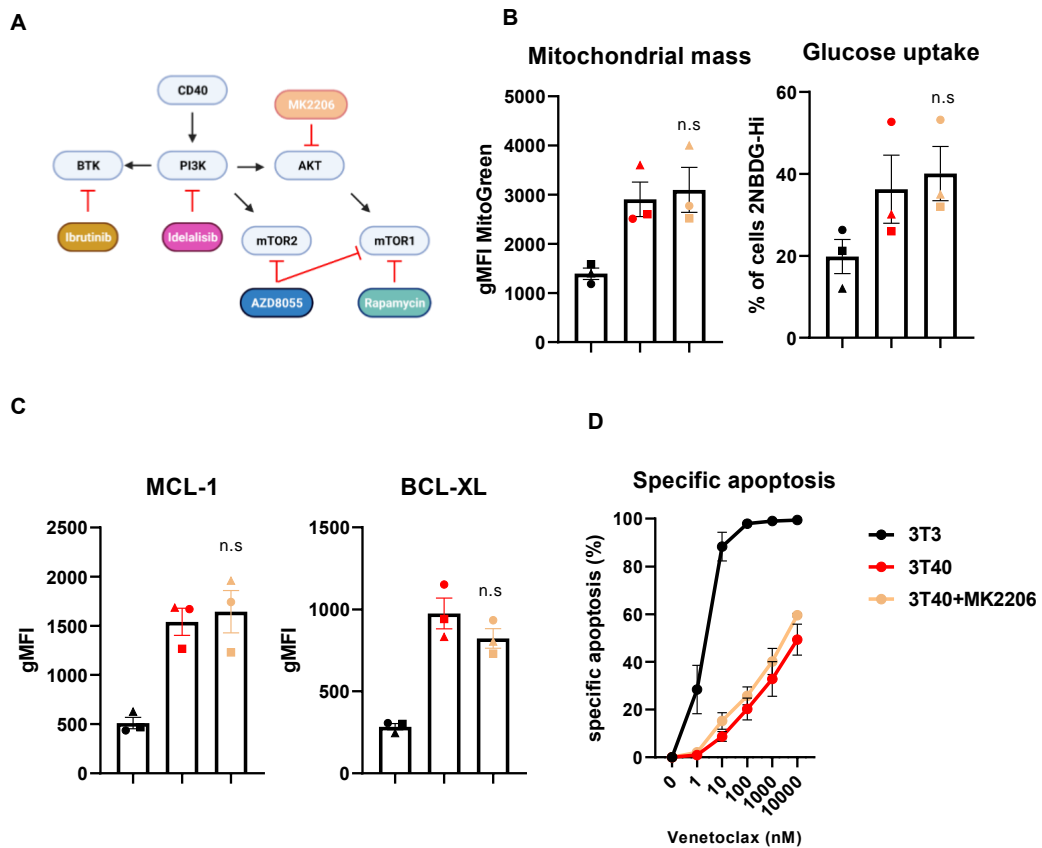


Figure S4. Effects of CD40 downstream regulators. (A) Schematic representation of inhibitors of downstream regulators of CD40 signaling and their inhibitors. (B) CLL cells were cultured on 3T3 or 3T40 fibroblasts and simultaneously treated with MK2206 (n=3) for 24 hours, after resuspension, mitochondrial mass and glucose uptake, (C) MCL-1 and BCL-XL were measured by flow cytometry. (D) After resuspension, CLL cells were then incubated with a titration of 1-10000 nM venetoclax for 24 hours after which viability was measured using MitoTracker Orange CMTMROS and TO-PRO-3, specific apoptosis was calculated (n=3). Data are shown as mean +/- SEM. One-Way ANOVA was performed to compare 3T40 to the other conditions. Each patient is labelled with a distinct symbol across all the conditions.

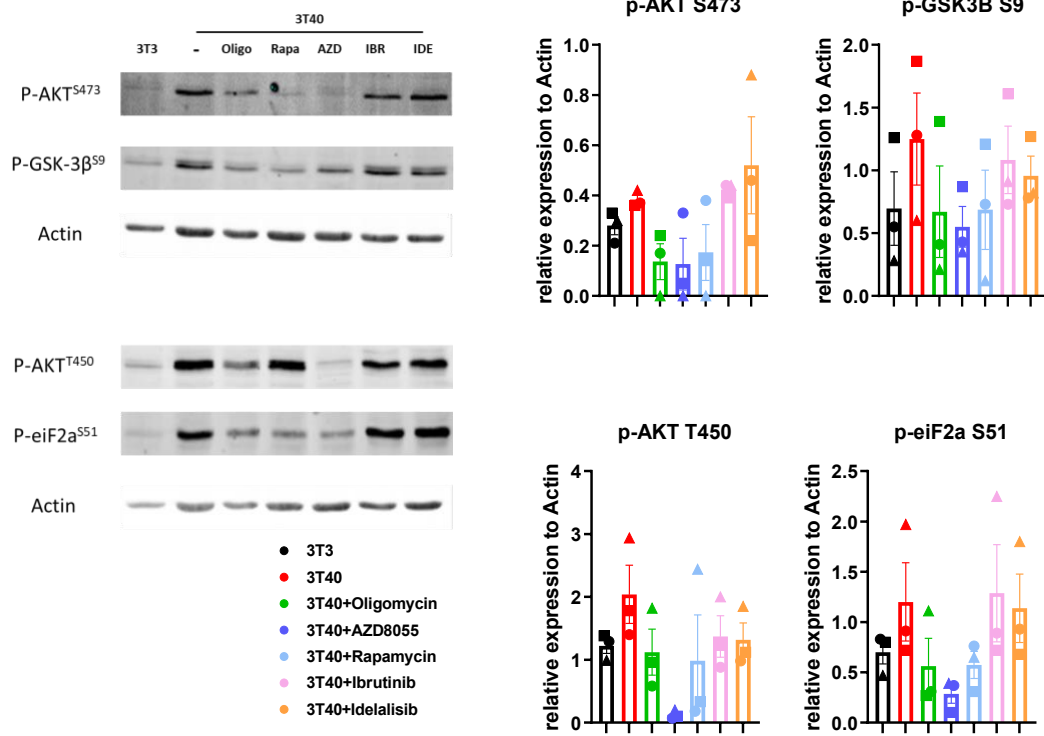


Figure S5. ETC inhibition cross talks to mTOR1/2 signalling. CLL cells (n=3) were cultured on 3T3 or 3T40 fibroblasts and simultaneously treated with Inhibitors of downstream regulators of CD40 signaling for 24 hours. After resuspension, protein expression of pAKT(S473), pGSK3 β (S9), pAKT(T450) and p-eif2 α (S51) were measured by western blot. Each patient is labelled with a distinct symbol across all the conditions.

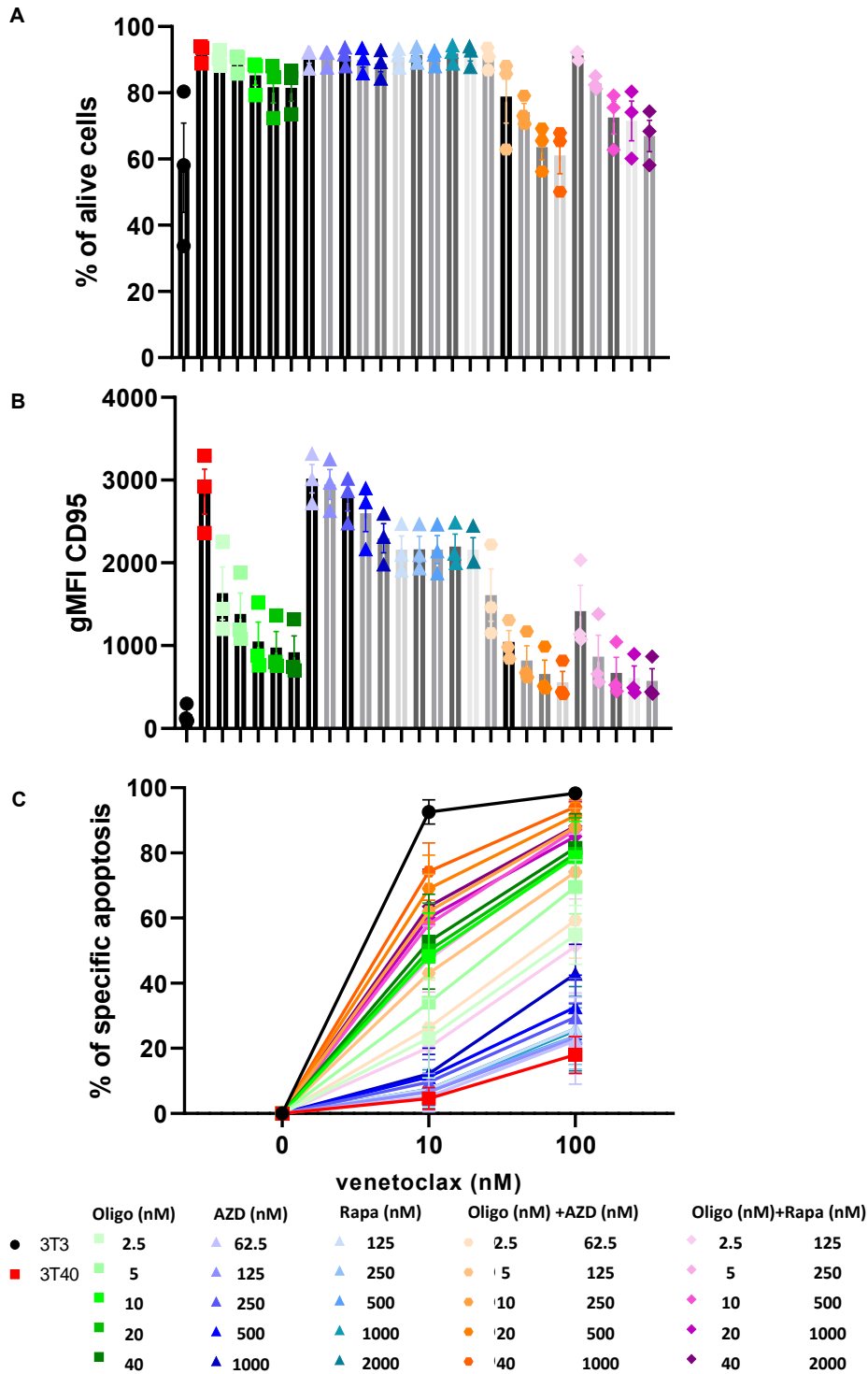


Figure S6. Synergy test of oligomycin and mTOR inhibitors. CLL cells (n=3) were cultured on 3T3 or 3T40L fibroblasts and simultaneously treated with various concentrations of oligomycin, AZD8055, rapamycin or combinations for 24 hours. After resuspension, (A) viability and (B) CD95 were measured by flow cytometry. (C) Cells were incubated with 10 or 100 nM venetoclax for 24 hours after which viability was measured using MitoTracker Orange CMTMROS and TO-PRO-3. specific apoptosis was calculated. Synergy score of ETC/mTOR inhibitors and venetoclax were calculated (From Figure S6C shown in Figure 6C).

Table S1. Patient table

	CLL number	IgHV status	WBC (x10 ⁹ /L)	% CLL	Therapy	Panel	
Figure 1	CLL01	Mutated		59.6	99.7 fludarabine+cyclophosphamide	A-C	
	CLL02	Unmutated		74.6	99.7 none	A-C	
	CLL03	Unmutated		121	99.8 fludarabine	A-C	
	CLL04	Unmutated		333.7	96.8 Bendamustine	D,E	
	CLL05	Unmutated		114.8	96.94 none	D,E	
	CLL06	Unmutated		207.23	96.03 none	D,E	
	CLL07	Unmutated		106.39	94.88 none	D,E	
	CLL08	Unmutated		80.25	95.02 none	D,E	
	CLL09	Unmutated		105.6	99.11 none	D,E	
Figure 2	CLL04	Unmutated		333.7	96.8 Bendamustine	A,C,D	
	CLL06	Unmutated		207.23	96.03 none	A-D	
	CLL07	Unmutated		106.39	94.88 none	A-D	
	CLL08	Unmutated		80.25	95.02 none	A-D	
	CLL09	Unmutated		105.6	99.11 none	A-D	
Figure 3	CLL10	Unmutated		148.7	95.21 none	A-C	
	CLL11	Unmutated		127.33	93.62 Bendamustine	A-C	
	CLL12	Mutated		58.51	92.26 none	A-E	
	CLL13	Mutated		56.31	93.93 none	A-D,F	
	CLL14	Mutated		253.8	94.48 fludarabine+cyclophosphamide+rituximab	A,B,E,F	
	CLL15	Mutated		100.9	89.01 none	A,B	
	CLL17	unknown		34.2	89.4 unknown	D	
	CLL08	Unmutated		80.25	95.02 none	D,E	
	CLL16	unknown		277.71	97.23 unknown	D,E	
	CLL09	Unmutated		105.6	99.11 none	D,E,F	
	CLL06	Unmutated		207.23	96.03 none	F	
Figure 4	CLL19	Mutated		68.9	88.4 rituximab+chlorambucil	A,C	
	CLL20	Mutated		135.74	96.14 none	A,C	
	CLL21	Unmutated		137.47	93.37 unknown	A,C	
	CLL06	Unmutated		207.23	96.03 none	B	
	CLL22	Mutated		89.92	95.68 none	B	
	CLL05	Unmutated		114.8	96.94 none	B	
	CLL23	Mutated		337.64	98.56 none	B	
	CLL24	Mutated		118.61	98.38 unknown	C	
	CLL25	Unmutated		88.8	97.79 fludarabine + cyclophosphamide + rituximab	C	
	CLL19	Mutated		68.9	88.4 rituximab+chlorambucil	A-C	
	CLL21	Unmutated		137.47	93.37 unknown	A-C	
	CLL08	Unmutated		80.25	95.02 none	B	
CLL12	Mutated		58.51	92.26 none	B		
CLL09	Unmutated		105.6	99.11 none	B		
CLL05	Unmutated		114.8	96.94 none	A,C		
CLL23	Mutated		337.64	98.56 none	A,C		
CLL20	Mutated		135.74	96.14 none	A,C		
CLL24	Mutated		118.61	98.38 unknown	C		
CLL25	Unmutated		88.8	97.79 fludarabine + cyclophosphamide + rituximab	C		
Figure 6	CLL21	Unmutated		137.47	93.37 unknown	A	
	CLL25	Unmutated		88.8	97.79 fludarabine + cyclophosphamide + rituximab	A-C	
	CLL24	Mutated		118.61	98.38 unknown	A-C	
	CLL26	Mutated		95.1	88.8 none	A	
	CLL23	Mutated		337.64	98.56 none	A-C	
Figure S1	CLL06	Unmutated		207.23	96.03 none	A-C	
	CLL02	Unmutated		74.6	99.7 none	B,C	
	CLL27	Mutated		113.3	93.5 none	B,C	
	CLL28	Mutated		83.8	93.5 none	B,C	
	CLL29	Mutated		43.4	94.1 none	B,C	
	CLL30	Unmutated		212	97.1 none	B,C	
	CLL31	Mutated		202	95 venetoclax	B,C	
	CLL32	Unmutated		170	95.6 unknown	B,C	
	CLL33	Unmutated		118.4	86.9 none	B,C	
	CLL34	Unmutated		46.69	92.34 none	B,C	
	CLL35	Unmutated		300.23	97.7 chlorambucil	B,C	
	CLL36	unknown		119	98 none	B,C	
	CLL16	unknown		277.71	97.23 unknown	D	
	CLL37	Unmutated		77.63	95.99 none	D	
	Figure S2	CLL06	Unmutated		207.23	96.03 none	A-E
		CLL07	Unmutated		106.39	94.88 none	A-E
		CLL08	Unmutated		80.25	95.02 none	A-E
CLL09		Unmutated		105.6	99.11 none	A-E	
Figure S3		CLL10	Unmutated		148.7	95.21 none	A,B
	CLL12	Mutated		58.51	92.26 none	A,B	
	CLL13	Mutated		56.31	93.93 none	A	
	CLL14	Mutated		253.8	94.48 fludarabine+cyclophosphamide+rituximab	A	
	CLL15	Mutated		100.9	89.01 none	A	
	CLL11	Unmutated		127.33	93.62 Bendamustine	B	
	CLL37	unknown		103.98	98.34 unknown	B	
	CLL06	Unmutated		207.23	96.03 none	C,D	
	CLL21	Unmutated		137.47	93.37 unknown	C,D	
	Figure S4	CLL19	Mutated		68.9	88.4 rituximab+chlorambucil	B-E
CLL20		Mutated		135.74	96.14 none	B-E	
CLL21		Unmutated		137.47	93.37 unknown	B-E	
CLL05		Unmutated		114.8	96.94 none	E	
CLL23		Mutated		337.64	98.56 none	E	
CLL06		Unmutated		207.23	96.03 none	E	
CLL22		Mutated		89.92	95.68 none	E	
Figure S5	CLL06	Unmutated		207.23	96.03 none		
	CLL23	Mutated		337.64	98.56 none		
	CLL22	Mutated		89.92	95.68 none		
Figure S6	CLL25	Unmutated		88.8	97.79 fludarabine + cyclophosphamide + rituximab	A-C	
	CLL24	Mutated		118.61	98.38 unknown	A-C	
	CLL23	Mutated		337.64	98.56 none	A-C	

Table S2. Reagents and products

Product	company	city	reference
Anti-BCL-XL	Cell signaling technology	Danvers, MA, USA	#12099
Anti-MCL-1	Cell signaling technology	Danvers, MA, USA	#656175
Anti-BCL2	Biolegend	San Diego, CA, USA	#658709
2-NBDG	Thermo Fisher scientific	Waltham, MA, USA	#N13195
Mito tracker green FM	Thermo Fisher scientific	Waltham, MA, USA	#M7514
MitoTracker Orange CMTMROS	Thermo Fisher scientific	Waltham, MA, USA	#M7510
DioC6	Thermo Fisher scientific	Waltham, MA, USA	#D273
Topro3	Thermo Fisher scientific	Waltham, MA, USA	#T3605
Anti-human CD19	BD biosciences	San Jose, CA, USA	#555415
Anti-human CD5	Biolegend	San Diego, CA, USA	#300620
Anti-human CD95	Biolegend	San Diego, CA, USA	#305621
fixable Viability dye e Fluor 780	Thermo Fisher scientific	Waltham, MA, USA	#65-0865-14
CytoFix/Cytoperm	BD biosciences	San Jose, CA, USA	#554722
Perm/Wash buffer	BD biosciences	San Jose, CA, USA	#54723
Fast SYBR green Master Mix	Thermo Fisher scientific	Waltham, MA, USA	#4385612
2DG	Merck	Darmstadt, DE	#D8375
Oligomycin	Merck	Darmstadt, DE	#O4876
Etomoxir	Tocris	Bristol, UK	#4539
Rotenone	Merck	Darmstadt, DE	#R8875
Antimycin A	Merck	Darmstadt, DE	#A8674
FCCP	Merck	Darmstadt, DE	#C2920
AZD8055	Selleckchem	Houston, TX, USA	#S1555
Rapamycin	Selleckchem	Houston, TX, USA	#S1039
MYLS22	MedChemExpress	Monmouth Junction, NJ , USA	#HY-136446
Idelalisib	Selleckchem	Houston, TX, USA	#S2226
MK2206	Selleckchem	Houston, TX, USA	#S1078
Ibrutinib	pharmacyclics	Sunnyvale, CA, USA	
DON	Selleckchem	Houston, TX, USA	#S8620
UK5099	Selleckchem	Houston, TX, USA	#S5317
DMM	Merck	Darmstadt, DE	#136441
Venetoclax	Bioconnect	Huissen, NL	#HY-15531
Poly-D-Lysine	Merck	Darmstadt, DE	#P6407
RPMI assay medium	Merck	Darmstadt, DE	#R1383
Actinomycin D	Merck	Darmstadt, DE	#A4262
Cyclohexamide	Merck	Darmstadt, DE	#01810
TriReagent	Merck	Darmstadt, DE	#93289
ATPlite kit	PerkinElmer	Waltham, MA, USA	#6016943
NAD+/NADH kit	Merck	Darmstadt, DE	#MAK037
RNeasy kit	Qiagen	Hilden, DE	#74104
RevertAid H Minus M-MuLV Reverse Transcriptase	Thermo Fisher scientific	Waltham, MA, USA	#EP0451
Anti-MCL1	Abcam	Cambridge,UK	#ab32087
Anti-CD40	Abcam	Cambridge,UK	#ab13545
Anti-Actin	SICGEN	Cantanhede, PT	#AB0145-200
Anti-P-AKT5473	Cell signaling Technology	Danvers, MA, USA	#9271
Anti-P-AKT450	Cell Signaling Technology	Danvers, MA, USA	#9267
Anti-P-GSK-3B59	Cell Signaling Technology	Danvers, MA, USA	#9323
Anti-P-eIF2a551	Cell Signaling Technology	Danvers, MA, USA	#3398
Click-IT assay kit	Thermo Fisher scientific	Waltham, MA, USA	#C10337

Table S3. Primers for qPCR

Gene	Forward primer	Reverse primer
CD40 Transcript 1	5'-CTGGTCTCACCTCGCTATGG-3'	5'-GCAGTGGGTGGTTCTGGAT-3'
CD40 Transcript 2 (alternatively spliced variant)	5'-TTGGACAAGGTCCCAGGAT-3'	5'-AGCACCAAGAGGATGGCAAA-3'
CELF1	5'-CCAGACAACCAGATCTTGATGCT-3'	5'-AGGTTTCATCTGTATAGGGTGATG-3'

References:

1. Haselager M V., Kielbassa K, ter Burg J, et al. Changes in Bcl-2 members after ibrutinib or venetoclax uncover functional hierarchy in determining resistance to venetoclax in CLL. *Blood* 2020;136(25):2918–2926.
2. Kielbassa K, Haselager M V., Bax DJC, et al. Ibrutinib sensitizes CLL cells to venetoclax by interrupting TLR9-induced CD40 upregulation and protein translation. *Leukemia* 2023;(December 2022):1–9.
3. Narayan RS, Molenaar P, Teng J, et al. A cancer drug atlas enables synergistic targeting of independent drug vulnerabilities. *Nat Commun* 2020;11(1):2935.
4. Van Attekum MHA, Terpstra S, Slinger E, et al. Macrophages confer survival signals via CCR1-dependent translational MCL-1 induction in chronic lymphocytic leukemia. *Oncogene* 2017;36(26):3651–3660.